Effect of Residual Monomer Content on Some Properties of a Poly(methyl methacrylate)-Based Bone Cement

C. I. VALLO, P. E. MONTEMARTINI, T. R. CUADRADO

Institute of Material Science and Technology (INTEMA), University of Mar del Plata and National Research Council (CONICET), J.B. Justo 4302, (7600) Mar del Plata, Argentina

Received 22 July 1997; accepted 3 January 1998

ABSTRACT: Through this article, the degree of polymerization attainable in a commercial acrylic bone cement based on poly(methyl methacrylate) (PMMA) was investigated by differential scanning calorimetry (DSC) and gas chromatography (GC). The results obtained revealed a marked dependence between the maximum monomer conversion and the cure temperature. Specimens for the mechanical evaluation of the cement were subjected to two different cure conditions: one set of samples was allowed to cure at room temperature and an additional set was also postcured at 140°C for 2 h. The latter thermal treatment permitted one to discard the presence of the unreacted monomer in the hardened material. The effect of the unreacted monomer on the mechanical behavior was evaluated by measuring the flexural modulus (E), the compressive yield stress (σ_y), and the fracture toughness (K_{IC}). Samples prepared at room temperature for mechanical evaluation contained residual monomer which acts as a plasticizer of the matrix, increasing K_{IC} and decreasing E and σ_y. The cure temperature and mold dimensions influence the amount of the residual monomer in the hardened material. Thus, differences in the values of the mechanical properties measured for the same commercial formulation may be attributed to a different mold dimension used in the test. © 1998 John Wiley & Sons, Inc. J Appl Polym Sci 69: 1367–1383, 1998

Key words: bone cements; PMMA; residual monomer; calorimetric study; postcuring; mechanical behavior

INTRODUCTION

Acrylic bone cement based on poly(methyl methacrylate) (PMMA) is used in orthopedics to fix both the femoral and acetabular components in a total hip replacement. Today, in most total joint replacements including the hip, knee, and ankle, acrylic bone cement is used as a means of fixation of the prosthesis to the bone. Bone cement is also often used in the fixation of pathological fractures and in the repair of bone defects.

PMMA enjoys wide industrial applications and is known as Plexiglas. The Plexiglas form of PMMA is heat-cured and formed under pressure. Although a vast amount of literature is available on the physical and mechanical properties of industrial PMMA, these are not directly applicable to bone cements. Surgical-grade PMMA is self-polymerizing and it is itself exothermic during curing. In fact, the temperature increase during the practical application in hip replacements varies between 50 and 80°C, depending on the thickness of the cement mantle.[1,2] Moreover, for surgical use, liquid methyl methacrylate (MMA) monomer is added and mixed with powdered PMMA polymer. After 3–5 min, the mix becomes doughlike and it is kneaded or worked by hand in

Correspondence to: C. I. Vallo.
Contract grant sponsor: National Research Council (CONICET).

Journal of Applied Polymer Science, Vol. 69, 1367–1383 (1998)
 CCC 0021-8995/98/071367-17

order to obtain a paste capable of being introduced into the cavity of the bone. After 12–15 min, the dough "sets up" into a rigid mass.[3] Toxic effects against cells and tissues caused by the presence of the MMA monomer have been reported in ref. 4. Nevertheless, these adverse factors occur only before and during polymerization, when MMA is in a high concentration. Cement, once polymerized, becomes a biocompatible material. For this reason, it is widely used for the fixation of prosthetic devices in orthopedic surgery.

Several authors[5–11] have studied various aspects of mechanical properties of bone cements. The effect of additives, the *in vivo* environment, porosity, radiopaque fillers, handling techniques, and molecular weight distribution upon mechanical properties have been the focus of much research attention. The hand-mixing of the components entraps bubbles, making the cement porous and much weaker under a load than is industrial PMMA. Porosity, pore size, and pore-size distribution were considered the main reasons for the lower strength of surgical-grade PMMA.[9–13]

Although the literature on bone cements is voluminous, relatively few studies have been reported on the effect of the residual monomer content on the mechanical evaluation of bone cements. The present work has two main objectives: the first objective was to study the degree of conversion attainable by the monomer under different curing conditions. For this purpose, the polymerization reaction was studied by differential scanning calorimetry (DSC) and gas chromatography (GC).

Thermal analysis has traditionally been used to characterize several properties of a wide array of materials among which polymeric materials are the most conspicuous. Among the thermal analysis techniques, differential scanning calorimetry (DSC) is the most popular and versatile technique. Whenever a material undergoes a change in a physical state, such as melting or glass transition, or whenever it reacts chemically, heat is either liberated or absorbed. Modern differential scanning calorimeters are designed to determine the enthalpies of these processes by measuring the heat flow required to maintain the sample material and an inert reference material at the same temperature. A unique feature of the use of the DSC thermal technique is the quantitative nature of the thermal data generated by the technique. Details of the theory and the design of differential scanning calorimeters were given by Turi.[14] Since the exothermic peak due to the cure reaction is accurately detected, DSC is a suitable technique to measure the heat liberated during the cure of the bone cement. DSC has the advantage that the degree of polymerization can be measured directly, assuming that the heat produced by the polymerization is proportional to the number of monomer units reacted.

Even though DSC is widely used in polymer research and characterization, few studies concerning the use of DSC for the evaluation of acrylic cements used in orthopedics and dentistry have been reported in the literature.[15–18] Through this article, the way in which this technique can be used for studying the curing reaction of bone cements was analyzed. The MMA polymerization was studied in both samples cured at constant temperatures and samples cured in the scanning mode at different heating rates.

Pascaud et al.[19] employed the DSC technique to analyze the degree of crystallinity and melting of ultrahigh molecular weight polyethylene, which is used as a bearing material for orthopedic devices. The authors reported that a problem that arose from the use of DSC is that the total energy measured during a test includes the energy to heat the air present in the gap between the sample and the cup walls. After the sample has melted, it takes the inner shape of the cup and the area of contact between the sample and its container is maximized so that the transfer of heat is enhanced. Hence, the differences observed in DSC traces between the first and second scan are attributed to the fact that in the second run the air has been excluded. This inaccuracy is discarded in the study of the cure of bone cements, because as a drop of liquid mixture is put into the sample holder, it takes the inner shape of the container immediately.

Gas chromatography (GC) was used in addition to the DSC measurements. GC is a suitable technique for the determination of the residual monomer content in the hardened cement. Provided that an appropriate column is used, the chromatograms of the samples analyzed show a peak which is clearly identified as the MMA monomer by comparison with MMA retention times of pure samples previously determined. The results of the use of this technique in the characterization of acrylic bone cements were reported by previous workers.[20,21]

The second objective of the present work was to investigate the influence of the residual monomer

content on some mechanical properties of a bone cement. For this purpose, the mechanical evaluation was performed on specimens subjected to two different cure conditions. One set of samples was allowed to cure at room temperature and an additional set was also postcured at 140°C for 2 h to induce complete reaction of the MMA monomer. The mechanical evaluation of the bone cement was accomplished by the measurement of flexural modulus of elasticity (E), compressive yield strength (σ_y), and fracture toughness (K_{IC}). These properties were selected because they are involved in critical situations of load under *in vivo* situations. Flexural properties are germane to the life of the arthroplasty because *in vivo* loading invariably involves a combination of shear, tension, and compression forces. On the other hand, in clinical service, the prosthesis is subjected to quasistatic direct compressive forces during certain activities, such as in a one-legged stance in the case of hip implants. Lee and Duckworth[22] and Ling and Duckworth[23] suggested that when a hip implant is anchored using bone cement the cement mantle may act as a compressive wedge, acting to drive the femoral stem apart from the bone. Quasistatic compressive properties of the bone cement are thus relevant. Moreover, the fracture toughness of the cement is clearly an important parameter as far as the prosthesis performance is concerned. This is because this parameter reflects the reliability and defect tolerance capability of the cement. Based on the proposition that when the cement is loaded in tension, cracks predominantly open in mode I and linear elastic conditions exist, the fracture toughness was obtained as the critical value of the mode I stress intensity factor (K_{IC}). This research aimed to give a further contribution to the understanding of the influence of the residual monomer upon the aforementioned mechanical properties of acrylic bone cements.

EXPERIMENTAL

Materials

For this study, a commercially available self-curing bone cement (noncrosslinked), Subiton (Subiton SRL, Buenos Aires, Argentina), kindly supplied by the manufacturers, was employed. Each dose of surgical bone cement consists of an envelope with 40 g of acrylic powder (P), sterilized with ethylene oxide, and an ampule with 20 g of the MMA monomer (L), sterilized by ultrafiltration. $BaSO_4$ is added to the powder to impart radiopacity to the cement. Table I shows the chemical ingredients of the radiopaque cement, as reported by the supplier. Cements are also manufactured with powder without $BaSO_4$, resulting in radiolucent cured materials.

Table I Manufacturer's Composition of Two-phase Bone Cement (Subiton)

Powder	Poly(methyl methacrylate)	35.03 g
	Benzoil peroxide	0.97 g
	Barium sulfate	4.00 g
Liquid	Methyl methacrylate	19.76 g
	N,N-Dimethyl-*p*-toluidine	0.24 g
	Hidroquinone	18–20 ppm

For most of this experimental work, the materials were prepared in a proportion of the components suggested by the manufacturer, that is, $L/P = 0.5$.[3] In addition, measurements of the temperature increases during polymerization and tests for the evaluation of mechanical properties were carried out in samples having an L/P ratio equal to 0.6. Samples with the MMA monomer without a chemical activator were prepared at room temperature and examined by scanning electron microscopy to obtain information of the structure of the material in the dough state, that is, before the initiation of the polymerization reaction.

Methods

Scanning Eletron Microscopy

The powder particles and the material in the dough state were examined by scanning electron microscopy (SEM) using a JEOL JSM 35 CF apparatus, after coating the surfaces with a thin gold layer.

Differential Scanning Calorimetry

The liquid–powder mixtures were prepared by hand mixing for 30 s at room temperature, in the proportion suggested by the manufacturer, that is, $L/P = 0.5$. Both components were prechilled at 5°C to prolong the working time, that is, to avoid a chemical reaction before the sample was properly loaded in the DSC equipment. Samples (8–10 mg) were sealed in hermetic aluminum

pans and tested immediately. The sample pans were reweighed after completion of the test to determine any loss of the monomer during the measurements.

Two different differential scanning calorimeters were used to measure the heat flow produced by the polymerization reaction as a function of time and temperature, after calibration with high-purity indium. The devices were a DuPont 990 provided with a 910 DSC cell and a Shimadzu TA 50 provided with a software which enables the data processing generated by each run. An empty capsule served as the reference. Runs were carried out under a nitrogen flow.

The instruments can be used isothermally at any predetermined temperature. In the case of a chemical reaction carried out at a constant temperature, a plot of heat output rate versus time is obtained. Alternatively, the instruments can be programmed to scan between two preset temperatures at a constant heating rate. In this case, a plot of heat output rate versus temperature is obtained. In both tests, the area under the exothermic peak is proportional to the heat released by the chemical reaction, that is, to the amount of monomer reacted.

In the DuPont device, isothermal runs are carried out, putting the sample into the cell once the instrument is in equilibrium at the preset test temperature. In this case, the sample reaches the test temperature immediately. In the Shimadzu device, isothermal measurements are performed, introducing the sample into the cell at room temperature and imposing a high heating rate until the temperature of interest is reached. In addition to the plot of heat output versus time or temperature, the Shimadzu device provides a register of the true temperature evolution in the sample. This information is very helpful in highly exothermic reactions, as it is the case of MMA polymerization, in which an overshooting may be produced, leading to an incorrect interpretation of the results.

Gas Chromatography

The peak height method was used to calculate the amount of unreacted monomer left in the system, which is in contrast to the principle used in the DSC measurement since DSC detects the amount of monomer reacted. One portion of approximately 2 g of the mixture was dispersed between two thin layers of aluminum, which were tightly sealed and immediately immersed in a temperature-controlled oil bath. In this way, films of a depth of approximately 1 mm were cured at constant temperature. Five temperatures, 39, 48, 63, 73, and 81°C, were used in the experiments. The cure times were set from the information provided by the isothermal DSC runs.

Approximately 1 g of the isothermally cured materials was weighed and dissolved in 25 mL of dichloromethane containing 0.1% of ethyl methacrylate as the internal standard. The mixture was shaken on a mechanical shaker until the polymer had completely dissolved.

The cured cement was analyzed in a Hewlett–Packard 5890 Series II gas chromatograph equipped with a flame ionization detector under the following experimental conditions: The columns used were 3 m length, 0.32 cm diameter stainless steel, 25% Emulphor 850 on Chromosorb W, with an acid-washed 80/100 mesh support. Injection port temperature was 140°C, detector temperature, 200°C; attenuation, 7, helium flow, 12 mL/min; hydrogen flow, 20 mL/min; and air flow, 300 mL/min. The column heating rate was 3°C/min from 35 to 100°C and 2°C/min from 100 to 150°C.

A 5-μL sample was injected into the gas chromatograph. The ratio of the monomer peak height to the ethyl methacrylate peak height was determined by each chromatogram. The monomer percentage in the cement specimen was determined from a least-squares line calibration curve constructed from detector response factors obtained from standard solutions containing 0.25, 0.5, 1, 2, 5, and 7.5% monomer. All determinations were conducted in triplicate.

Gel Permeation Chromatography

The molecular weight distributions were determined in both the powder and the hardened material using a Waters ALC/GPC 244 apparatus with a differential refractive index detector. Samples of the original radiopaque powder and the cured material prepared in a proportion L/P equal to 0.5 were dissolved in tetrahydrofuran at 0.1% (wt/vol) and were subsequently subjected to size-exclusion gel permeation chromatography. The weight-average (M_w) and number-average (M_n) molecular weights were determined from the retention time using a calibration curve with a polystyrene standard. Samples of the cured material were taken from the test specimens used in the fracture toughness testing.

Temperature Evolution During the Cure in Molds

The temperature increase caused by the highly exothermic reaction was measured during the cure of the resins in both rectangular and cylindrical molds. Temperature changes during polymerization were followed by the insertion of a copper-constantant thermocouple into the molds. The thermocouples were connected to a digital multimeter which displays the voltage values every 0.4 s with an accuracy of $\pm 0.05\%$. The thermoelectric voltage values were visually read from the liquid crystal display of the multimeter at intervals of 5 s. Thermoelectric voltages were converted into temperatures using a copper-constantant thermocouple reference table. Temperatures were corrected by taking into account that the standard error of the thermocouple is 0.75%. The measurements were performed in duplicate. In these cases, a radiolucent cement was used to determine the precise position of the thermocouple recording tip in relation to the acrylic mass.

The cement mass influences the temperature reached during curing due to the highly exothermic MMA polymerization. Hence, differences in curing temperature that arose from the differences in mold geometry or variations in the L/P ratio may be expected to occur. Rectangular molds consisted of two glass plaques spaced by rubber cords of different diameters and held together with clamps. In this way, plaques of different thicknesses were obtained, which allowed the evaluation of the effect of the thickness of the cement mantle on the maximum temperature reached. Cylindrical molds consisted of polypropylene disposable tubes of 80-mm length and internal diameters equal to 6 and 30 mm. Additionally, samples with an L/P ratio equal to 0.6 were made in order to evaluate the effect of the component proportions on the temperature evolution during polymerization.

Mechanical Properties

The mechanical properties measured were the flexural modulus of elasticity (E), the compressive yield strength (σ_y), and the fracture toughness (K_{IC}). A radiolucent cement was used to eliminate the effect of $BaSO_4$ particles upon the mechanical behavior. All samples were prepared in the same way to avoid the eventual influence of the preparation technique upon the mechanical properties. Both components, that is, liquid and powder, were prechilled at 5°C before mixing and then mixed slowly by hand for 0.5 min. Following mixing, the cement was poured immediately into molds to prepare specimens for subsequent mechanical characterization. All samples were allowed to cure at room temperature. In the case of compression and fracture specimens, one set was also postcured at 140°C for 2 h to induce complete chemical reaction of the MMA monomer.

Mechanical testings were carried out at room temperature in a Shimadzu Autograph S-500-C universal testing machine at a crosshead displacement rate of 2 mm/min. Plates for flexure and fracture specimens were obtained by casting the mixture into molds consisting of two rectangular glass plaques spaced by a rubber cord and held together with clamps. Test specimens were produced by cutting slabs into beams using a diamond saw.

Samples for compression testing were made by injecting the mix into polypropylene cylindrical disposable molds of 6-mm internal diameter. After removal from the molds, the compression specimens were machined to reach the final dimensions. The Young's modulus was measured in flexure. The results were computed using the standard formula:

$$E = L^3P/4bd^3y$$

where E is the Young's modulus; L, the length between supports; P, the load; b, the width of the specimen; d, the thickness of the specimen; and y, the deflection at the center. Flexural moduli were determined using sample dimensions recommended by ASTM D790. The results are the average of eight measurements.

The surgical PMMA cement is brittle in nature. Like other brittle materials, it is weak in tension but quite strong in compression[24] and capable of yielding under uniaxial compression. So, yield strength was determined in compression. Cylindrical specimens having an aspect ratio of 2 were deformed between metallic plates lubricated with molybdenum disulfide. True stress-deformation curves were obtained by dividing the load by the original cross-sectional area and converting it into true stress, assuming constant volume deformation. The deformation was calculated directly from the crosshead speed. The yield stress was determined at the maximum load.[25] The effect of the proportion of the components upon the compressive behavior was studied by performing mea-

surements in samples with an L/P equal to 0.5 and 0.6.

Fracture mechanic measurements were made in three-point bending in samples prepared with the proportion used in the practical application, that is, $L/P = 0.5$. The fracture toughness of each cement was characterized through the critical stress intensity factor, K_{IC}, calculated from

$$K_{IC} = \sigma_c(\pi a)^{1/2} f(a/W)$$

where $\sigma_c = 3P_cL/(2b^2W)$ is the critical stress for crack propagation; P_c, the load at fracture; L, the span between supports; b, the thickness; W, the width; a, the initial crack length; and $f(a/W)$, a calibration factor. For this geometry, $f(a/W)$ is given by[26]

$$f(a/W) = 1.09 - 1.735\,(a/W) + 8.2\,(a/W)^2 - 14.18\,(a/W)^3 + 14.57\,(a/W)^4$$

Central V notches were machined in the bars and extended by tapping a fresh razor blade into the tip of the notch to give a crack length range of $0.45 < a/W < 0.55$. The span-to-width (L/W) ratio was always kept equal to 4. The length of the initial crack, a, was measured from the fracture surface using a profile projector with a magnification of 10, averaging the results in five points as suggested by ASTM E399 standard. K_{IC} was determined from the slope of a plot of $\sigma_c(\pi a)^{1/2}$ versus $1/f(a/W)$, obtained from at least 12 specimens.

RESULTS AND DISCUSSION

Scanning Electron Microscopy

Figure 1(a,b) shows the morphology of the powder with and without a radiopacifier. In the first case, it is observed that the powder consists of spherical particles ranging in size from 10 to 50 μm. In the powder with the radiopacifier, the barium sulfate is seen covering the PMMA particles. In the material in the dough state [Fig. 1(c,d)], the PMMA particles are seen bound together with a significant grade of cohesion. Pascual et al.[7] studied the influence of the size and size distribution of the PMMA powder component in the curing of classical bone cement formulations. The authors proposed that PMMA particles could play a strong role in the polymerization reaction. From their point of view, PMMA beads with a diameter larger than 60–70 μ are not dissolved by MMA, but particles of smaller diameters could be readily dissolved by the monomer before reaching the dough state. The SEM study of the cement used in this work reveals that in the case of dissolution of the PMMA powder by the monomer the dissolution is only partial and even the smallest particles retain their identity. The differences between the morphology of this cement and the cements studied by Pascual et al. may arise from differences in the molecular weight of the powders. From the SEM micrograph, it emerges that the polymerized material consists of spheres of PMMA bound by a matrix of PMMA produced by the polymerization reaction of the MMA monomer.

Degree of Cure Measured by DSC and GC

The objective of this experiment was to determine the presence of unreacted monomer in the hardened cement as well as the effect of the cure temperature on the degree of MMA polymerization. For this purpose, samples were cured inside the DSC cell isothermally between 20 and 80°C at intervals of 10°C. Once the isothermal cure was completed, the samples were quenched and scanned from 20 to 150°C at a heating rate of 10°C/min. The variation of the rate of heat output as a function of time and temperature was obtained on a chart recorder. All specimens were reweighed after the scans and no material loss was detected.

In Figure 2(a–c), typical DSC thermograms are presented. Figure 2(a) is a plot of the heat output rate versus time of a sample cured isothermally at 30°C. The reaction started after an induction time. The time required for the completion of the cure was determined when the rate curve leveled off at the baseline very close to the initial baseline. Figure 2(b) is a thermogram of a second scan at 10°C/min in which the presence of a residual exhoterm is observed. These results are explained by the fact that with increasing conversions of the monomer during the isothermal cure a point was reached where the solution of the polymer in the monomer became a glass. Vitrification was attained when the glass transition temperature (T_g) of the sample reached the cure temperature. In a glass, even small molecules have extremely low mobility, and for practical purposes, the reaction rate is zero in the normal reaction

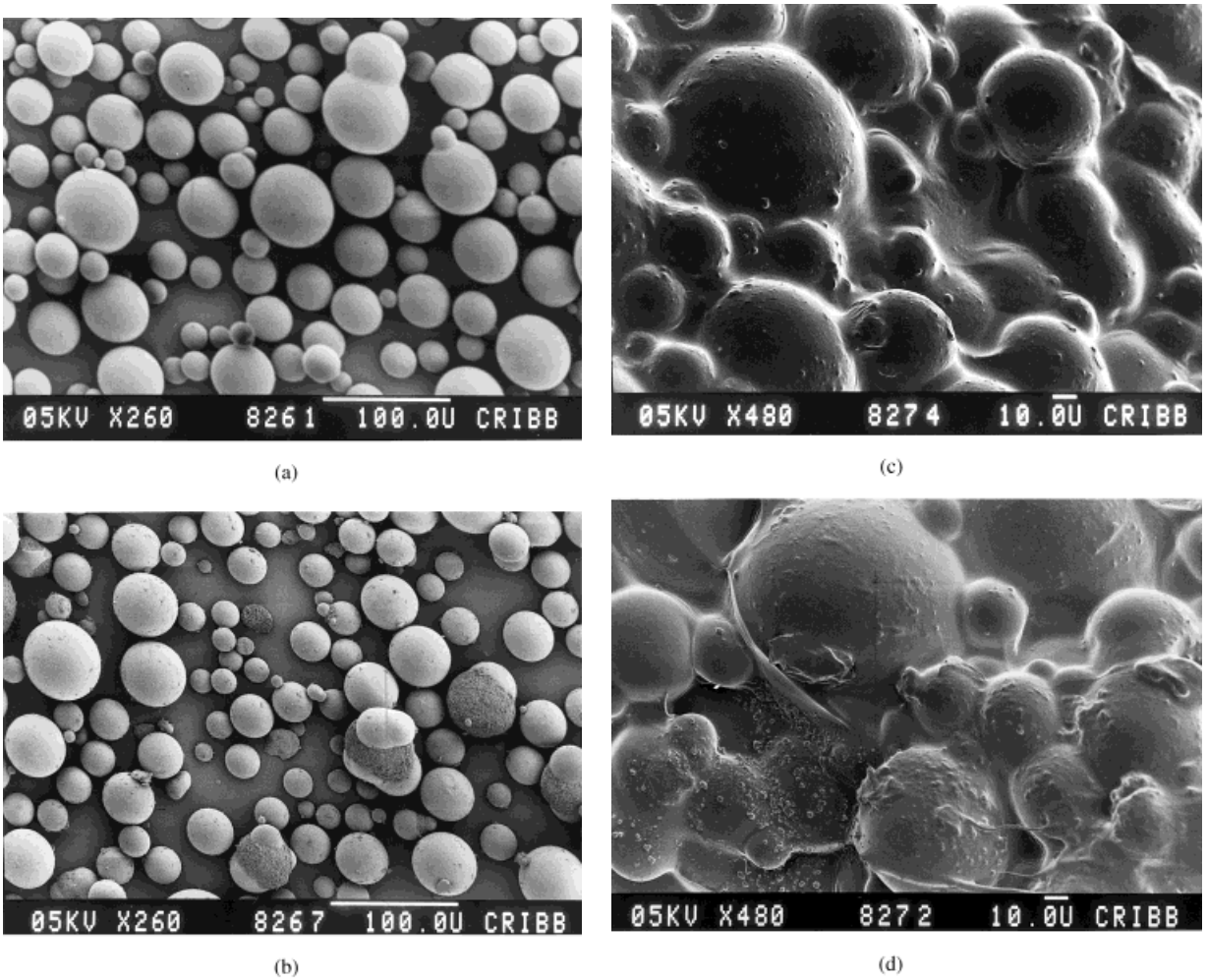

Figure 1 (a) Scanning electron micrograph of powder component of the radiolucent cement. (b) Scanning electron micrograph of powder component of the radiopaque cement. (c,d) Scanning electron micrographs of the radiopaque cement in the dough state.

time scale. The residual exothermic peak present in the second scan of the sample [Fig. 2(b)] is the reaction heat not released during the isothermal curing because vitrification prevented the curing reaction from going to completion. The additional inflection overlapped at the end of the exothermic peak corresponds to the T_g of the PMMA powder particles. The superposition of the exothermic peak with the T_g of the powder phase made it impossible to calculate accurately the residual heat of the remaining reaction. Several baselines were tried, but the results obtained had a high dispersion. Figure 2(c) shows a third scan of the sample from 20 to 150°C at a heating rate of 10°C/min. The absence of a residual exothermic peak is observed and the inflection corresponds to the glass transition temperature of the cured sample. This T_g is the same as the T_g measured for the PMMA powder present in the bone cement, which is 110°C.

Some observations related to the DSC technique are worth noting. In isothermal runs carried out at low cure temperatures, the sample was at constant temperature during the whole run, but at temperatures higher than 50°C, an overshooting was observed. This is shown in Figure 3(a,b). The curves correspond to isothermal runs carried out at 30 and 50°C in the Shimadzu apparatus.

As the test temperature was obtained by first heating the sample from room temperature to the

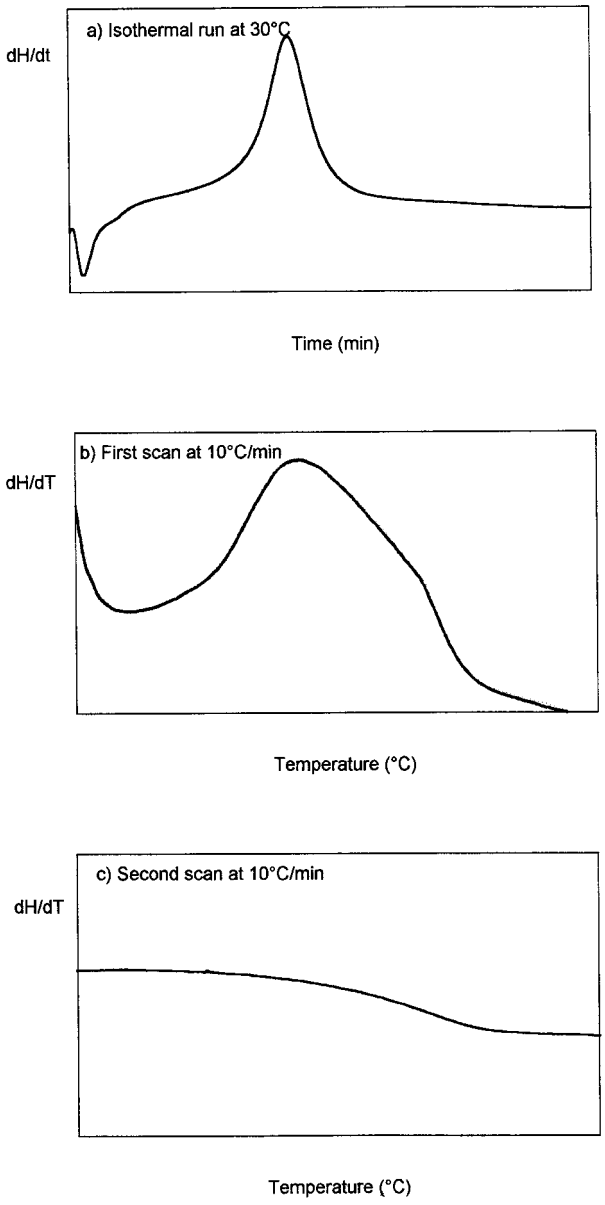

Figure 2 Samples subjected to (a) isothermal cure at 30°C, (b) first scan at 10°C/min, and (c) second scan at 10°C/min.

test temperature at a high heating rate, in samples cured at 50°C, part of the reaction took place during the heating period. As a consequence, there was a loss of information, that is, an inaccuracy in the measurements. Several initial heating rates between 20 and 90°C/min were used to avoid a reaction during the heating stage, but in no case was an isothermal cure obtained. On the other hand, in the DuPont apparatus, a lack of thermal equilibrium during the first stage of the reaction was also observed at temperatures higher than 50°C. From these results, it emerges that the DSC technique in the isothermal mode gives accurate results only for temperatures below 50°C.

DSC in the isothermal mode has been used to study the cure reaction of acrylic cements used in dentistry as restorative and cavity-lining materials. Heats of reaction, monomer conversion, and kinetic parameters have been accurately determined by Tryson and Schultz,[15] McCabe and Wilson,[16] Eliades et al.,[17] and Vaidyanathan and Vaidyanathan.[18] As in these particular applications a small amount of cement is required, the temperature increase during cure is between 40 and 50°C. Hence, the results reported by the authors were in the range of temperatures where the technique provides accurate results.

In orthopedic applications, temperatures lower than 50°C are reached in cases that require a small mass of material, as it is the fixation of metacarpophalangeal and interphalangeal joint

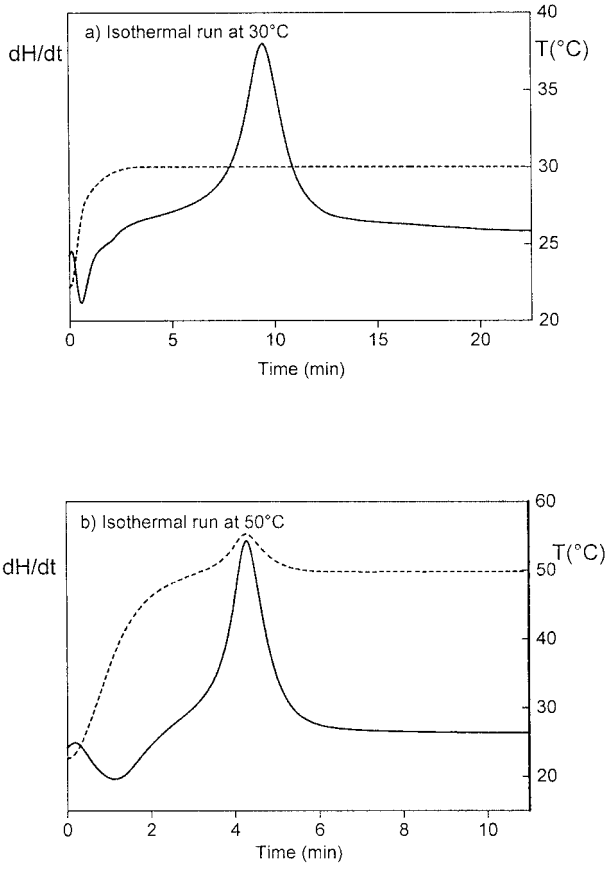

Figure 3 Samples subjected to (a) isothermal cure at 30°C and (b) isothermal cure at 50°C.

Table II Residual Monomer in Samples Isothermally Cured Determined by Gas Chromatography

Temperature (°C)	W (%)	W^* (%)	X
39	6.4 (±0.1)	19.2 (±0.3)	0.81 (±0.003)
48	5.5 (±0.1)	16.5 (±0.3)	0.835 (±0.003)
63	4.2 (±0.2)	12.6 (±0.6)	0.875 (±0.006)
73	3.5 (±0.15)	10.5 (±0.4)	0.895 (±0.004)
81	2.5 (±0.2)	7.5 (±0.6)	0.925 (±0.006)

prostheses with acrylic bone cement.[27] However, during a hip replacement, the temperature increase varies between 50 and 80°C.[1–2] Consequently, in this practical application, it is important to obtain information about the behavior of the cure reaction in a larger range of temperatures than that provided by the isothermal DSC runs. Due to the aforementioned experimental inaccuracies, the residual monomer content present in the hardened cement was determined by GC. Samples were cured isothermally in a temperature-controlled oil bath at 39, 48, 63, 73, and 81°C. In spite of the drawbacks of DSC when it is used isothermally at temperatures higher than 50°C, the technique provides useful information as regards the vitrification time during the cure under isothermal conditions. In fact, the cure time was set according to the vitrification time previously determined by DSC.

From the GC experimental results, the following quantities may be calculated: W, the weight fraction of the unreacted monomer based on the total mass, that is, liquid and powder (in a proportion $L/P = 0.5$), and W^*, the weight fraction of unreacted monomer based on the monomer weight present in the initial mixture. As the molecular weight of the MMA is 100 g/mol, the conversion of the monomer, X, is $X = (1 - W^*/100)$.

Table II gives the values of W, W^*, and X obtained for each determination. Figure 4 shows the weight fraction of the remaining monomer based on the initial amount of MMA, W^*, versus the cure temperature. It represents the effect of the polymerization temperature on the limiting conversion. The results reported by Balke and Hamielec[28] for the polymerization of PMMA in bulk are presented in the same plot. A good concordance is observed between the maximum degree of the reaction for MMA polymerization in the bulk and the maximum degree of the reaction measured in this work for the MMA polymerization in the acrylic bone cement. The residual monomer in the bone cement is, on average, 7% higher than the correspondent to the bulk polymerization. This suggests that in this proportion of the components the particles of PMMA present in the cement have little effect on the maximum conversion attained by the MMA monomer.

The influence of the L/P ratio on the maximum degree of the reaction was studied in samples having L/P ratios equal to 0.5 and 0.6. The residual monomer was determined by a method of sample preparation reported by Brawer et al.[20] The mixtures were placed in a silver ring (diameter 20 mm, height 2 mm) covered with two glass plaques. In samples of this thickness, it may be assumed that a uniform temperature profile during polymerization is attained. The resins were allowed to cure at room temperature, and after 24 h, a portion of approximately 1 g of the cured material was dissolved in 25 mL of dichloromethane. The experimental results of the monomer content de-

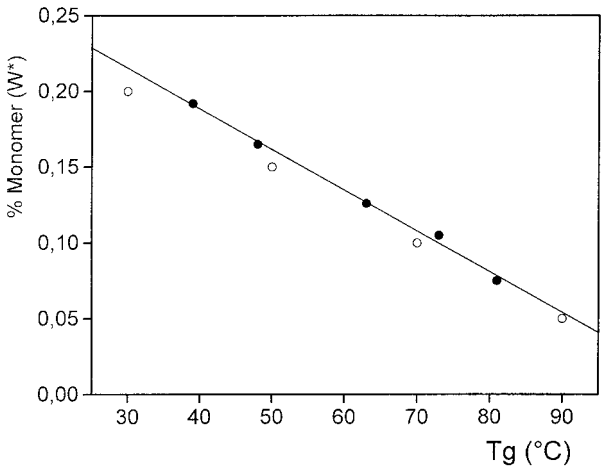

Figure 4 Residual monomer content measured by GC in samples isothermally cured. The hollow points correspond to the polymerization of MMA in bulk reported by ref. 28.

Table III Residual Monomer Content in Samples Prepared with Different *L/P* Ratios

L/P	*W* (%)	*W** (%)	Conversion *X*
0.5	5.9 (±0.2)	17.7 (±0.6)	0.82 (±0.006)
0.6	4.7 (±0.2)	12.5 (±0.5)	0.87 (±0.005)

termined by gas chromatographic analysis are outlined in Table III. From the results obtained, it emerges that samples having a higher L/P ratio reached a higher degree of MMA conversion. The results may be explained by taking into account that the smaller powder proportion used in the samples with $L/P = 0.6$ produces a mixture with a lower initial viscosity and a higher monomer content by volume unit, leading to a higher degree of monomer conversion.

The curing reaction was also investigated by DSC in a dynamic mode. Nonisothermal DSC measurements provide useful information over a broad temperature range. As the test starts at room temperature, inaccuracies during the first period of the cure are not present. Experiments were performed at heating rates of 2, 5, 7.5, 10, 15, and 20°C/min in the range 20–150°C. The reaction was considered to be complete when the rate curve leveled off to the baseline. DSC thermograms obtained at different heating rates are shown in Figure 5(a,b). At low heating rates, the rate curve leveled off to the initial baseline at temperatures below 80°C. In these cases, the baseline was accurately defined. However, at heating rates higher than 10°C/min, there was an overlapping of the curve of the reaction rate with the T_g of the PMMA particles. This complicated the calculus of the total heat evolved, estimated from the area

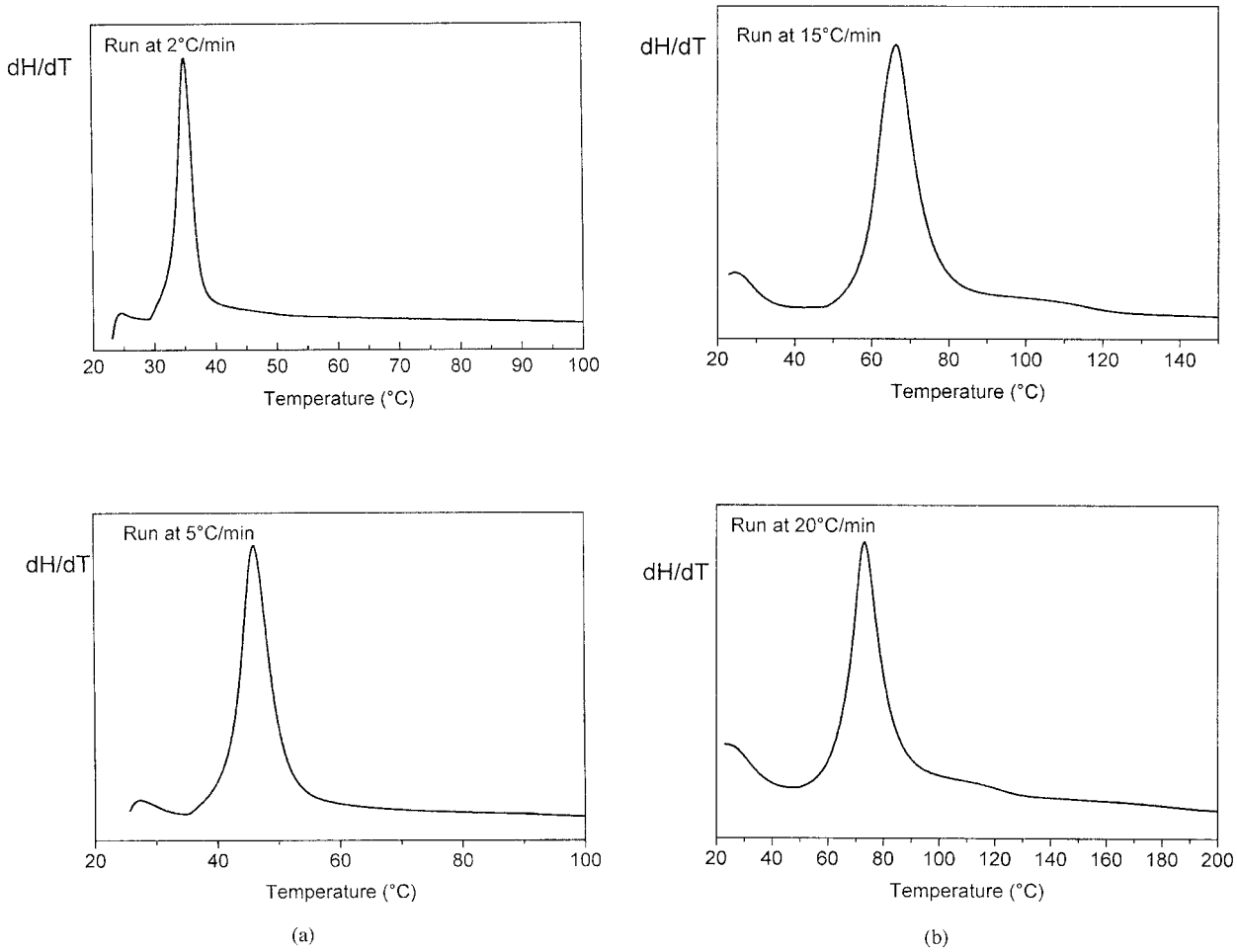

Figure 5 (a) DSC thermograms obtained in runs at 2 and 5°C/min. (b) DSC thermograms obtained in runs at 15 and 20°C/min.

Table IV ΔHu Values Detected by DSC at Different Heating Rates

Heating Rate q (°C/min)	ΔHu (kJ/mol)	Conversion X
2	46.6 (±0.4)	0.82 (±0.007)
5	47.4 (±0.5)	0.84 (±0.008)
7.5	49.6 (±0.7)	0.87 (±0.012)

under the exothermic peak. For this reason, the heat released by the reaction was solely calculated on the runs in which the baseline was properly determined by integrating the dH/dt–temperature curve. In this way, the total heat detected by DSC runs (ΔHu) was calculated. The total heat evolved during MMA polymerization at 100% conversion, ΔHr, is 56,9 kJ/mol.[14] Table IV gives the results for ΔHu calculated at different heating rates and the maximum conversion detected, X, defined as

$$X = (\Delta Hu)/(\Delta Hr)$$

The results shown in Table IV indicate that the values obtained for ΔHu were lower than for ΔHr, from which it emerges that an incomplete conversion of the monomer was attained. At low heating rates, kinetic limitations are not present and the incomplete conversion of the monomer during the test is explained by the diffusion-controlled reaction in free-radical MMA polymerization.[28]

The extent of cure, X, versus temperature for the scans performed at low heating rates was calculated by

$$X = (1/\Delta Hr) \int (dH/dT)\, dT$$

The results are presented in Figure 6. The polymerization starts at a very high rate after the inhibitor was consumed and it is stopped by the diffusion control of the reaction. It is observed that the vitrification curve is attained before completing the reaction. The chemical process is rapid but the diffusive process is slow, so the chemical reaction takes place only as fast as the reactants can diffuse together. In a region close to the vitrification, the reaction rate slows down abruptly, but as heating proceeds, temperature continues to increase. Then, the conversion follows a trajectory bounded by the vitrification curve.

From DSC and GC determinations, it emerges that due to the vitrification phenomenon the polymerization ceases before consuming the available MMA monomer. Furthermore, it was demonstrated that there are remarkable differences in the maximum monomer conversion among the cements cured at different temperatures.

Molecular Weight Characterization

Table V gives the number- and weight-average molecular weights as well as the ratio $D = M_w/M_n$ made on both the original powder and the final product. D is a parameter indicative of molecular weight distribution. When D is large, the weight-average molecular weight differs widely from the number-average molecular weight and the molecular weight distribution is broad. According to the results given in Table V, the values of D for the powder and the hardened material are similar. The lower molecular weight of the cured resin compared with the powder indicates that the matrix which forms on polymerization of the liquid portion of the mix has a lower molecular weight than that of the powder particles which it cements together.

Commercial heat-cured PMMA has generally a higher molecular weight than was found for the self-curing resin. Thus, it is not surprising that the industrial grades have better physical properties. However, for the rapid diffusion of the monomer and the swelling of the powder consistent with appropriate doughing times, a comparatively

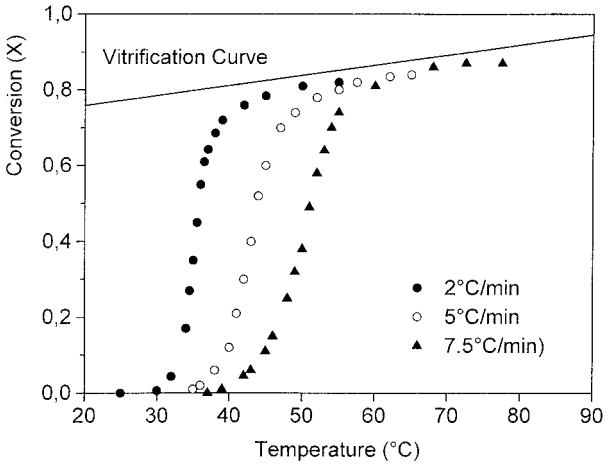

Figure 6 Conversion versus temperature in dynamic runs carried out at low heating rates.

Table V Molecular Weights of Powder and Cured Materials

Material	M_n	M_w	$D = M_w/M_n$
Powder	310,073 (±5%)	807,635 (±5%)	2.60
Cured	241,507 (±5%)	688,198 (±5%)	2.77

low molecular weight PMMA powder is a desirable ingredient for bone cements.

Temperature Evolution During the Cure in Molds

The purpose of this experiment was to measure the temperature increase caused by the heat production as well as the influence of the mold geometry and the dimensions on the temperature evolution during the polymerization. The initial temperature of the components affects the time to reach the dough stage. As the material was prechilled before molding, the time in which the maximum is observed is delayed with respect to that established by the manufacturer for the application in the surgical environment.[3]

Figure 7 shows the experimental measurement of the temperature evolution during the curing in rectangular molds. The maximum temperature reached increases to a high degree according to the thickness of the cement mantle. As the thickness becomes smaller, the peak temperature becomes less. On the other hand, the temperature actually recorded by a thermocouple depends on the precise position of its recording tip in relation to the acrylic mass. Figure 8 shows the differences in the recorded temperatures for a cement mantle of a thickness of 6 mm when the thermocouple is placed in the center and in the wall of the mold. A difference of as little as a 3 mm in the position of the thermocouple tip can produce a highly significant change in the temperature recorded.

Figure 9 gives the temperature increases measured during polymerization in cylindrical molds. According to the results given in Figure 9, it is clear that the peak temperatures in the center of the cement masses are related primarily to their volume. Temperatures of 100°C were reached in the middle of the cylinder measuring 30 × 80 mm.

The temperature evolution during the cure of the materials having L/P proportions equal to 0.5 and 0.6 in cylindrical molds of 6-mm internal diameter is shown in Figure 10. An increasing L/P ratio increases the inhibitor/initiator ratio, which delays the beginning of the polymerization process. As was expected, the maximum temperature reached increased with the L/P ratio.

It has been postulated that bone cement has a

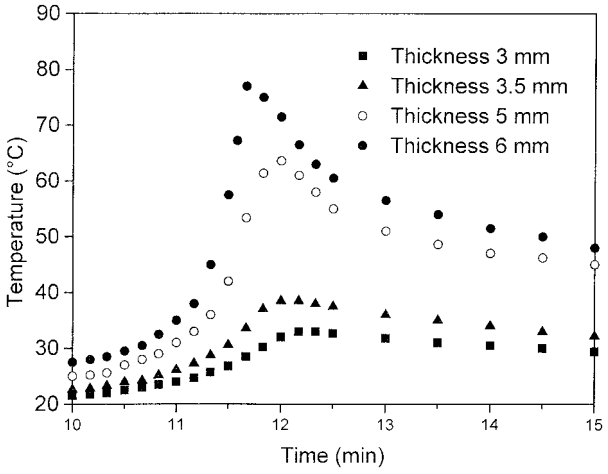

Figure 7 Evolution of the temperature during the cure in rectangular molds of different thickness.

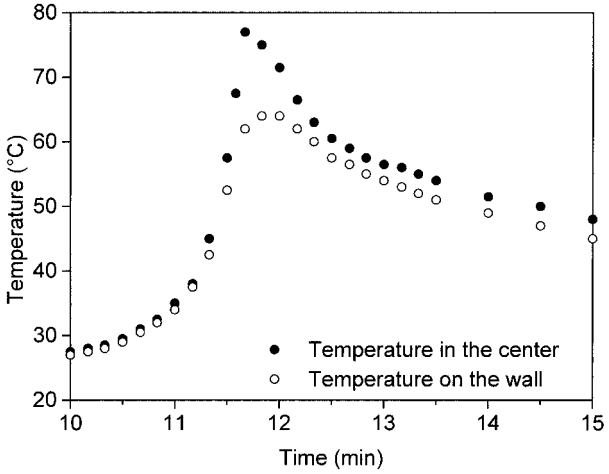

Figure 8 Differences recorded in the temperature evolution when the thermocouple is placed in the center or on the wall of the mold. The cure was carried out in a rectangular mold of a thickness of 6 mm.

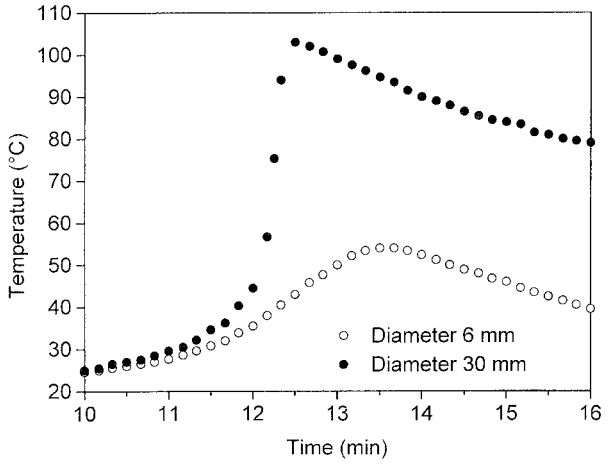

Figure 9 Evolution of the temperature during the cure in cylindrical molds of internal diameters equal to 6 and 30 mm.

role in the thermal necrosis of the adjacent bone, which is attributed to the high temperatures reached during polymerization. The results obtained in the present experiment show that temperatures reached in the cement mantle are in the range 60–80°C, which is higher than the temperature that produces bone necrosis.[29] The temperature evolution during polymerization depends on the rate of heat production and the rate of heat transference to the surroundings through the conduction and convection mechanisms. Consequently, the temperature reached at the interface bone/cement is related primarily to the surface area of the interface and the thermal properties and temperature of the surroundings. As the molds in which the temperature evolution was measured differ markedly from the bone cavity, to extrapolate the laboratory measurement results to a clinical situation such as a cemented arthroplasty would be merely speculative.

From the results obtained in this experiment, it emerges that during the cure of the resin a temperature profile across the mantle thickness is produced. The thicker the specimen, the higher the difference between the temperature reached in the center and the temperature reached in the wall. The nonuniform distribution of the temperature results in a nonuniform distribution of the monomer content because the polymerization is stopped by vitrification at different temperature values. Furthermore, different peak temperatures that arose from different mold dimensions may be correlated with different monomer contents in the hardened cement.

Mechanical Properties

Mechanical properties were measured under different testing modes to investigate the effect of the residual monomer content upon the mechanical behavior. Even though this work focused mainly on the effect of the residual monomer content on some mechanical properties, it is worth noting some aspects related to the sample preparation. It is widely recognized that there are two types of pores in fully polymerized bone cements: macropores (pore diameter >1 mm) and micropores (pore diameter $\approx 0.1-1$ mm). Prechilling of the components before mixing has been advocated as a means of decreasing the porosity of the cement.[8–10] To compare the effect of the storage temperature of the components on the porosity of the hardened cement, samples were prepared with components stored at both room temperature and 5°C. The use of a radiolucent cement allowed the evaluation of the pore size by visual inspection. In cements prepared with prechilled components, the porosity was markedly reduced and the presence of macropores was not observed. The results demonstrated that prechilling of the components prior to mixing is an effective means of decreasing the porosity of the fully polymerized material. Thus, prechilling is recommended in the

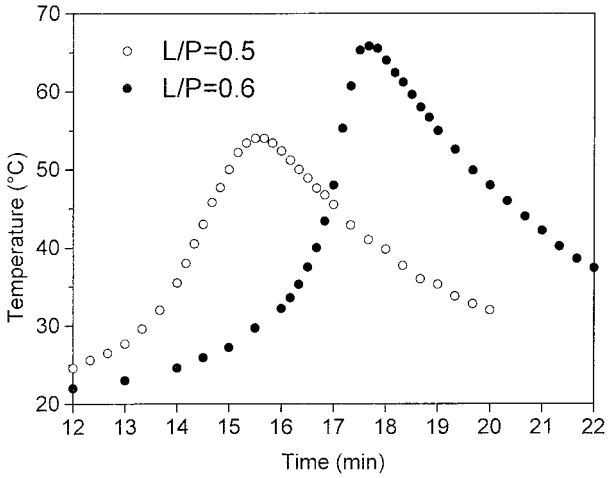

Figure 10 Evolution of the temperature during the cure in samples having L/P ratios equal to 0.5 and 0.6. The cure was carried out in cylindrical molds of an 6-mm internal diameter.

Table VI Young's Modulus, *E*, and Maximum Cure Temperature, T_{max}, in Specimens of Different Thickness

Thickness (mm)	T_{max} (°C)	*E* (GPa)
4	51	1.92 ± 0.12
5	64	2.27 ± 0.08

clinical practice such as in a cemented arthroplasty.

Flexural moduli were measured in specimens of 4 and 5 mm in thickness to determine if the Young's modulus measured in three-point bending is affected by the sample thickness. As was shown in Figure 7, the evolution of the temperature during the cure in the rectangular molds is greatly affected by the thickness of the mold. Hence, different monomer contents may be expected in samples that reached different peak temperatures. The results obtained are given in Table VI. It is observed that there is a marked dependence between the flexural modulus with the thickness of the test specimens. The explanation of this behavior is that the thinnest specimens, which cured at lower temperature, had a higher monomer content, resulting in a more flexible material. Lewis[9] reviewed the results of the *in vitro* determinations of the flexural modulus of six commercial formulations of bone cements. Although the determinations have been carried out in accordance with the ASTM D790 or ISO 5833 specifications, various specimen sizes ranging from 5 × 6 × 50 to 10 × 10 × 110 mm have been used. The differences in the flexural modulus values reported may be a consequence of different monomer contents that arose from different specimen dimensions.

As was described in the Experimental section, compression and fracture tests were performed on specimens subjected to two different curing conditions. One set was allowed to cure at room temperature and an additional set was also postcured for 2 h at 140°C. The latter treatment permits one to discard the presence of the residual monomer in the hardened materials. Thus, the influence of the monomer was evaluated by comparing the mechanical behavior of cements having different monomer contents.

Figures 11 and 12 show the results of compression tests carried out on samples having L/P ratios equal to 0.5 and 0.6 subjected to the aforementioned curing conditions. By comparing σ_y values, it clearly emerges that the free monomer present in samples cured at room temperature acts as a matrix plasticizer, leading to lower compressive yield stress values.

The influence of the L/P ratio can also be evaluated from this test. Samples with $L/P = 0.6$ displayed a lower porosity than did samples with $L/P = 0.5$, which is consistent with its lower initial viscosity that allowed the bubbles embodied during mixing to escape. The void proportion was verified visually by direct observation with a light microscope. No effort was made to quantify these observations, but the solely visual inspection revealed a marked difference in porosity between the samples. In addition, the gas chromatographic analysis revealed that samples with a higher L/P ratio resulted in materials with a lower monomer content (Table III). From these observations, the fall in σ_y values displayed by the specimens having the highest L/P ratio is explained in terms

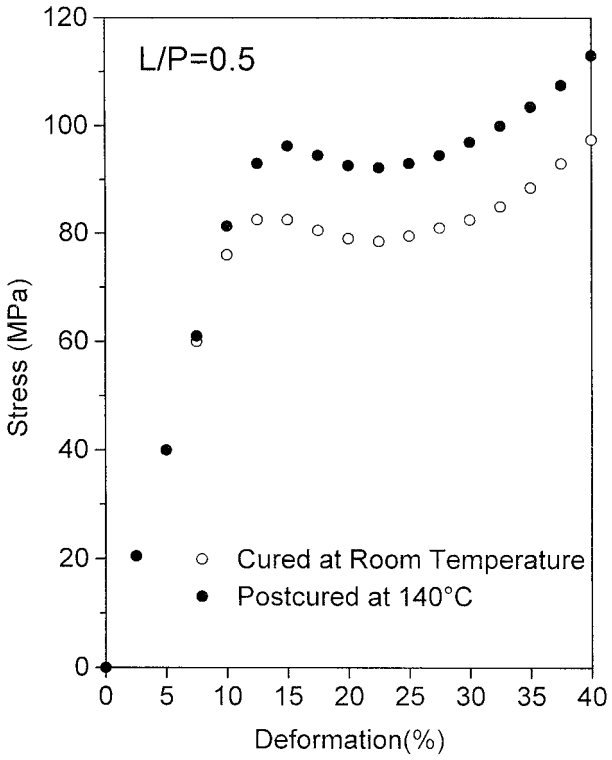

Figure 11 Stress versus nominal strain in the uniaxial compression test for specimens having an L/P ratio equal to 0.5. The tests were performed in samples cured at room temperature and in samples postcured at 140°C.

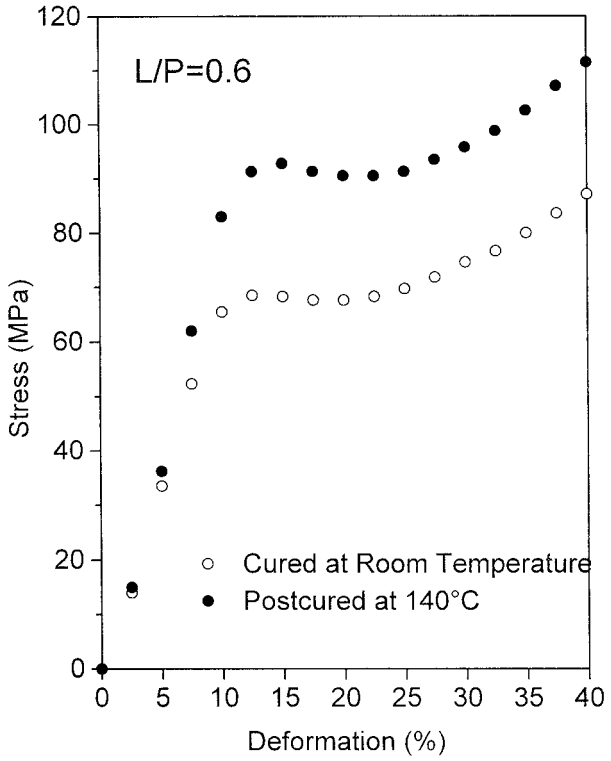

Figure 12 Stress versus nominal strain in the uniaxial compression test for specimens having an L/P ratio equal to 0.6. The tests were performed in samples cured at room temperature and in samples postcured at 140°C.

of less PMMA powder content, which acts as a reinforcement.

Table VII outlines the values of the fracture toughness and yield stress measured on samples having the component proportion used in the practical application, that is, $L/P = 0.5$. From the analysis of Table VII, it emerges that materials cured at room temperature displayed higher KIC values than did materials postcured at 140°C. On the other hand, K_{IC} increases when σ_y decreases. The results are consistent with the following hypothesis: The presence of a residual monomer content in the acrylic matrix in samples cured at room temperature leads to a blunting at the crack tip. When yielding occurs at a lower stress, an increase in the size of the plastic zone at the crack tip is expected. This blunting at the crack tip tends to improve material toughness. The materials cured at 140°C, which are practically free of the unreacted monomer, displayed a lower K_{IC} value, in accordance to the increase in σ_y.

The results of these experiments indicate that specimens of acrylic bone cements molded and cured at room temperature contain unreacted monomer due to an incomplete cure. As the polymerization took place at temperatures below the T_g at 100% conversion, the vitrification phenomenon limited the maximum conversion of the MMA monomer.

At this point, it is relevant to discuss some experimental results reported by previous workers. Brawer et al.[20] measured the residual monomer content in the hardened material by gas chromatographic analysis and they found that even after storage in air or water for many months it contained unreacted MMA. The authors reported 2.7% of free monomer for samples stored in air 20 h after mixing. On further storage in air, the monomer concentration decreased only slowly and reached a value of 2.4% after 215 days. If samples were stored in water at 37°C without stirring, the monomer was leached out and the MMA content was reduced to 1.4% after 4–5 months. These results clearly demonstrate that the hardened material contains an amount of unreacted monomer that evaporates or leaches over time.

Some authors[9] reported results of measurements of the mechanical properties in samples stored under different conditions, that is, in air at room temperature, in air at 37°C, in distilled water at 37°C, and in bovine serum at 37°C. The rate of diffusion of the residual monomer by leaching into the storage medium depends on the characteristics and temperature of the storage medium. Thus, the value of a property is markedly affected by the storing medium and temperature

Table VII K_{IC} and σ_y in Cements with L/P = 0.5 Cured at Room Temperature and Postcured at 140°C

Cure Cycle	σ_y (MPa)	K_{IC} (MPa $m^{1/2}$)
Cured at room temperature	82.5 ± 2	1.24 ± 0.04
Postcured at 140°C	96 ± 3	1.12 ± 0.03

as well as by the time elapsed between the preparation and the testing of the specimens. The different monomer content present in the specimens subjected to different storing conditions may be the cause of the scatter in the value of a property measured for a same commercial formulation.[9] The results shown in this experimental work permit one to evaluate the influence of the residual monomer content in the hardened cement upon some selected mechanical properties. As samples were prepared in the same way, porosity is not a parameter to take into account in samples having the same L/P ratio and the differences in the values of the properties can solely be attributed to differences in monomer content which was varied through different thermal treatments. On the other hand, it was demonstrated that sample dimensions influence the value of the properties because a different sample size gives, as a result, a different amount of monomer in the hardened material.

CONCLUSIONS

The degree of monomer conversion in a PMMA-based bone cement is limited by the vitrification phenomenon. From data obtained by gas chromatographic analysis, the vitrification of the resin was represented in a conversion versus temperature diagram, which can be used to estimate the limiting conversion of the monomer. Specimens simply cured at room temperature contain unreacted monomer that produces an increase in K_{IC} and a decrease in σ_y due to its plasticizer effect.

The maximum temperature reached during polymerization in rectangular molds showed a marked dependence on the thickness of the molds. The different temperature profiles produced during polymerization result in hardened materials with different amounts of unreacted monomer. Consequently, differences in the mechanical property values reported for a same commercial formulation may be attributed to a different monomer content in the test specimens made of different dimensions.

As Lewis[9] pointed out, the key parameters that influence the mechanical behavior of acrylic bone cements are cement formulation, mixing method, porosity, and aging conditions. From the results shown in the present work, it emerges that test specimen dimensions have an important role because different sample sizes result in hardened cements with different monomer contents.

The financial support provided by the National Research Council (CONICET) is gratefully acknowledged. Appreciation is extended to Mr. Hector Asencio for his assistance in preparing samples for mechanical characterization.

REFERENCES

1. S. Harving, K. Soballe, and C. Bünger, *Acta Orthop. Scand.,* **62,** 546 (1991).
2. J. S. Wang, H. Franzén, S. Toksvig-Larsen, and L. Lidgren, *J. Appl. Biomater.,* **6,** 105 (1995).
3. PROTHOPLAST S.A.I.C. Especialidades Medicinales Aprobadas por el Ministerio de Salud y Acción Social, Certificado No. 38.692.
4. T. Kindt-Larsen, D. Smith, and J. S. Jensen, *J. Appl. Biomater.,* **6,** 75 (1995).
5. S. Saha and S. Pal, *J. Biomed. Mater. Res.,* **18,** 435 (1984).
6. J. L. Hailey, I. G. Turner, A. W. Miles, and G. Price, in *11th European Conference on Biomaterials,* Pisa, Italy, Sept. 10–14, 1994, pp. 317–320.
7. B. Pascual, I. Castellano, B. Vázquez, I. Goni, M. Gurruchaga, M. P. Ginebra, F. J. Gil, J. A. Planell, B. Levenfeld, and J. San Roman, in *11th European Conference on Biomaterials,* Pisa, Italy, Sept. 1994, pp. 1–4.
8. G. Lewis and G. Austin, *J. Appl. Biomater.,* **5,** 307 (1994).
9. G. Lewis, *J. Appl. Biomater.,* **38,** 155 (1997).
10. G. Lewis, J. S. Nyman, and H. H. Trieu, *J. Appl. Biomater.,* **38,** 221 (1997).
11. P. Müllwe-Wille, J. S. Wang, and L. Lidgren, *J. Appl. Biomater.,* **38,** 135 (1997).
12. S. P. James, T. P. Schmalzried, F. J. McGarry, and W. H. Harris, *J. Biomed. Mater. Res.,* **27,** 71 (1993).
13. J. S. Wang, S. Toksvig-Larsen, P. Müller-Wille, and H. Franzén, *J. Biomed. Mater. Res. (Appl. Biomater.),* **33,** 115 (1996).
14. A. Turi, Ed., *Thermal Characterization of Polymeric Materials,* Academic Press, London, 1981.
15. G. R. Tryson and R. Schultz, *J. Polym. Sci. Polym. Phys. Ed.,* **17,** 2059 (1979).
16. J. F. McCabe and H. J. Wilson, *J. Oral Rehab.,* **7,** 103 (1980).
17. G. C. Eliades, G. J. Vougiouklakis, and A. A. Caputo, *Dent. Mater.,* **3,** 19 (1987).
18. J. Vaidyanathan and T. K. Vaidyanathan, *IEEE Trans. Biomed. Eng.,* **38,** 319 (1991).
19. R. S. Pascaud, W. T. Evans, P. J. J. MnCullagh,

and D. FitzPatric, *J. Biomed. Mater. Res.,* **32,** 619 (1996).
20. G. M. Brawer, D. J. Termini, and G. C. Dickson, *J. Biomed. Mater. Res.,* **11,** 577 (1977).
21. R. P. Kusy, *J. Biomed. Mater. Res.,* **12,** 271 (1978).
22. A. J. Lee and T. Duckworth, Eds., in *Proceedings of the Symposium on Revision Arthroplasty,* 2nd ed. Franklin, London, 1983, p. 8.
23. R. S. Ling and T. Duckworth, Eds., in *Proceedings of the Symposium on Revision Arthroplasty,* 2nd ed., Franklin, London, 1983, p. 14.
24. R. P. Kusy and D. T. Turner, *Polymer,* **18,** 391 (1977).
25. P. B. Bowden and J. A. Jukes, *J. Mater. Sci.,* **3,** 183 (1968).
26. A. J. Kinloch and R. J. Young, *Fracture Behavior of Polymers,* Applied Science, Essex, England, 1983.
27. R. J. Schultz, A. D. Johnston, and S. Krishnamurty, *Int. Orthop.,* **11,** 277 (1987).
28. S. T. Balke and A. E. Hamielec, *J. Appl. Polym. Sci.,* **17,** 905 (1973).
29. Swenson, D. J. Schurman, and R. L. Piziali, *J. Biomed. Mater. Res.,* **15,** 83 (1981).